

Image Generation as a Visual Planner for Robotic Manipulation

Pang Ye

Southern China University of Technology
Guangzhou, China

202264690373@mail.scut.edu.cn

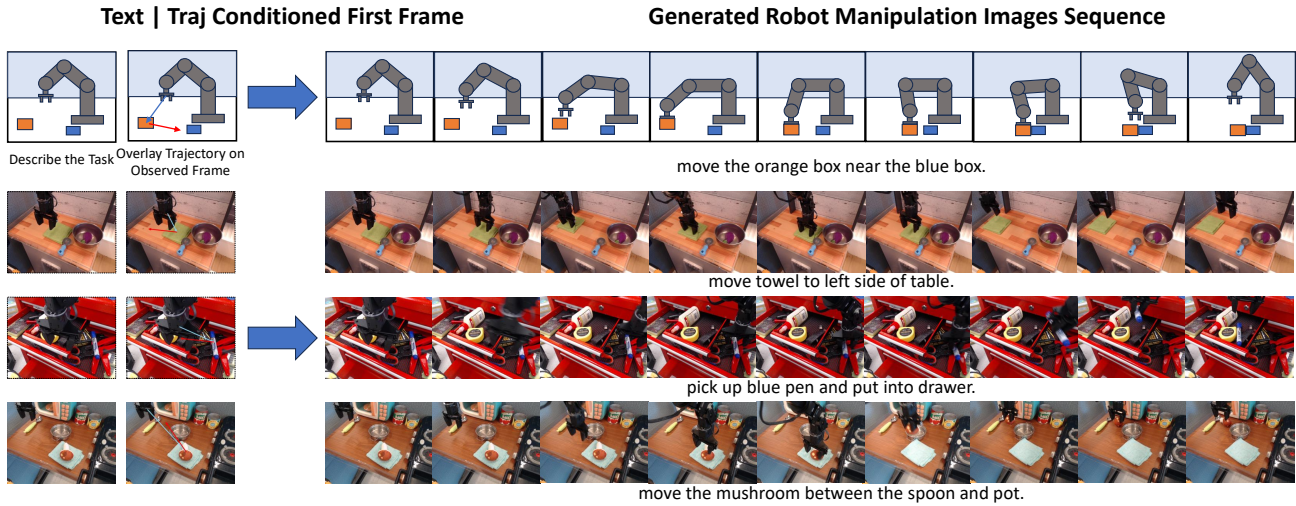


Figure 1. **Overview of our work.** We convert a pretrained image generator into a visual planner that synthesizes 3×3 manipulation grids under either text or trajectory conditioning.

Abstract

Generating realistic robotic manipulation videos is a key step toward unifying perception, planning, and action in embodied agents. While existing video diffusion models require large domain-specific datasets and struggle to generalize, recent image generation models trained on language-image corpora exhibit strong compositionality—including the ability to synthesize temporally coherent grid images. This suggests a latent capacity for video-like generation even without explicit temporal modeling.

We explore whether such models can serve as visual planners for robots when lightly adapted via LoRA fine-tuning. We propose a two-part framework with: (1) **text-conditioned generation**, using a language instruction and the first frame; and (2) **trajectory-conditioned generation**, using a 2D trajectory overlay and the same initial frame. Experiments on **Jaco Play dataset**, **Bridge V2** and **RT1 dataset** show that both modes produce smooth, coherent robot videos aligned with their respective conditions.

Our findings indicate that pretrained image generators encode transferable temporal priors and can serve as video-like robotic planners under minimal supervision. Code is released at <https://github.com/pangye202264690373/Image-Generation-as-a-Visual-Planner-for-Robotic-Manipulation>.

1. Introduction

Generating realistic *robotic manipulation videos* is a fundamental challenge for embodied intelligence and robot planning. A model capable of visually imagining how a robot executes a high-level instruction—e.g., “pick up the red cup and place it on the table”—would bridge perception, planning, and action in a unified manner. Such a capability enables robots to reason about future states and physical interactions directly in the visual domain.

However, learning to synthesize coherent robot videos

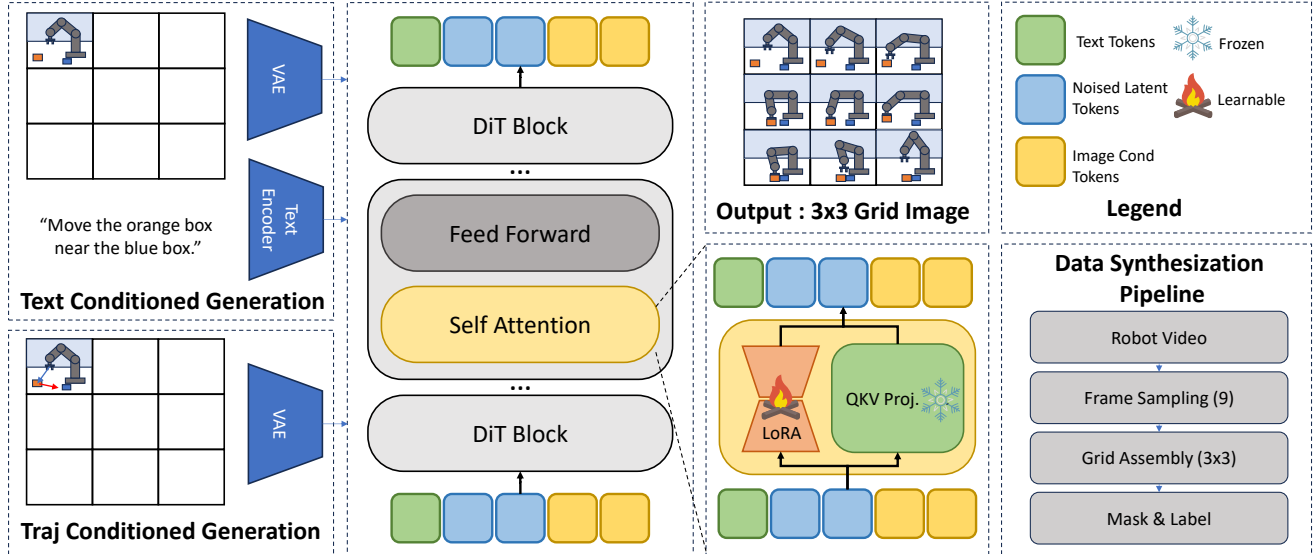


Figure 2. **Overall framework of our approach.** Our method adapts a pretrained image generator (DiT backbone with LoRA adapters) into a controllable video-like synthesizer that outputs a 3×3 grid image representing a short manipulation sequence. The upper branch shows the *text-conditioned* generation, where a language instruction and the first observed frame are encoded by the Text Encoder and VAE respectively. The lower branch shows the *trajectory-conditioned* generation, where a 2D path is rendered over the first frame and encoded similarly. Both branches share the same DiT architecture with LoRA applied to attention projections. On the right, the data synthesis pipeline illustrates how robot videos are processed: frame sampling, grid assembly, and masking for conditional supervision. On the right, the data synthesis pipeline illustrates how robot videos are processed: frame sampling, grid assembly, and masking for conditional supervision. See fig 3 for details.

remains difficult. Existing video diffusion or action-conditioned models require large-scale domain-specific robot datasets and often fail to generalize beyond seen tasks or scenes. Their heavy temporal modeling also leads to high computational cost and limited semantic understanding.

Meanwhile, modern *image generation models* such as diffusion or transformer-based architectures have achieved remarkable progress in realism and semantic alignment after training on billions of language–image pairs. Beyond single-frame synthesis, these models exhibit strong *compositional generation* capabilities: they can arrange multiple coherent images within a single grid layout, preserving spatial and semantic consistency across sub-images. Interestingly, such grids often resemble step-by-step visual progressions—akin to short video clips—with implicit temporal transitions between neighboring cells. This phenomenon reveals that image generators may already contain latent capacity for *video-like generation*, even without explicit temporal modeling. Such visual coherence, compositionality, and physical plausibility are precisely the ingredients required for robotic planning.

Thus, pretrained image generators already possess rich priors over objects, physics, and composition—qualities that are essential for robotic planning.

Motivated by these observations, we hypothesize that

large-scale image generation models can act as *visual planners* for robots, capable of synthesizing temporally coherent manipulation sequences from minimal conditional cues. Instead of designing new video architectures, we explore how existing image generators can be adapted, via lightweight **LoRA**-based [15] finetuning, to produce robot manipulation videos guided by simple conditions, as shown in figure 1.

Our exploration consists of two complementary parts:

1. **Text-Conditioned Generation (Text + First Frame).** In the first setting, the model receives a natural-language instruction together with the first observed image of the robot and environment. Through LoRA adaptation, it learns to generate temporally coherent sequences that visually execute the instruction. This experiment studies the model’s ability to perform *text-following*—understanding high-level semantics and transforming them into plausible motion imagery.
2. **Trajectory-Conditioned Generation (Trajectory + First Frame).** In the second setting, the model is conditioned on a rendered 2D end-effector trajectory over the initial frame, along with the same first image. The model learns to follow the provided spatial guidance while maintaining physical consistency, emphasizing *trajectory-following*—precise, continuous

control of robot motion through visual synthesis.

Together, these two paradigms investigate complementary aspects of generative control: semantic reasoning through language versus spatial reasoning through motion trajectories. They reveal how large-scale image generators can be repurposed as *video-like robotic planners* when provided with appropriate conditioning signals.

Experimental highlights. We evaluate both paradigms on multiple robotic video datasets, including **JacoPlay**, **Bridge**, and **RT1 datasets**. Our adapted models produce smooth, semantically aligned motion sequences that follow their respective conditioning modalities. The text-conditioned model generalizes to unseen instructions, while the trajectory-conditioned model excels at spatial precision. Both outperform task-specific video diffusion baselines in perceptual quality and action fidelity

Contributions. We summarize our main contributions as follows:

- **Image Generation as Visual planning.** We reveal that pretrained image generation models, known for producing coherent grid images, can be adapted to serve as *video-like planners* for robotic manipulation.
- **Two-part Conditional Framework.** We introduce a lightweight LoRA-based adaptation with two complementary conditioning modes—*text + first frame* and *trajectory + first frame*—enabling both semantic and spatial control.
- **Comprehensive Evaluation and Insights.** Extensive experiments show strong text-following and trajectory-following performance across datasets, highlighting how these conditioning forms jointly enable visual reasoning and motion synthesis.

Our framework builds on a standard diffusion/DiT backbone with LoRA adapters for conditioning, trained under first-frame supervision and autoregressive decoding.

2. Related Work

Image Generation Models. Diffusion models have become the de facto approach for high-fidelity image synthesis. Diffusion Transformers (DiT) replace the U-Net backbone with a Transformer and set strong image generation performance on ImageNet, cementing the “Transformerization” of diffusion backbones [37]. For controllability, ControlNet adds a zero-initialized control branch on top of a frozen text-to-image backbone to inject spatial hints such as edges, depth, or human pose, substantially improving composition and layout control [53]. While these advances establish powerful *static* image controllability, bridging from compositional control in single images to *temporally consistent* and *task-aligned* control in videos remains challenging—motivating us to adapt DiT-style models to robotic manipulation videos.

Video Generation and Diffusion. Recent text-to-video (T2V) progress shows rapid improvements in temporal coherence and long-range consistency [1, 11, 19, 21, 25–30, 32, 35, 38, 39, 54]. *Lumiere* proposes a single space–time U-Net that generates the full video in one pass, improving cross-frame consistency compared to keyframe-then-upsampling pipelines [2]. OpenAI’s *Sora* demonstrates sustained object persistence and long-horizon dynamics under text prompts, reinforcing the emerging view of video generators as “world simulators” [34]. Surveys synthesize the design space and challenges of diffusion-based video generation, including temporal modeling and evaluation [31]. Yet generic T2V models still struggle with *precise* motion and interaction constraints. To address this, trajectory-/tracking-conditioned video diffusion has emerged: TrackDiffusion conditions on multi-object tracklets for instance-consistent motion control [22], while Motion Prompting conditions on sparse/dense point trajectories to jointly control object and camera motion [12]. These trends suggest that explicit spatiotemporal constraints are key to pushing video diffusion from “compelling visuals” to *task-usable* generations—exactly the regime required for robot manipulation videos.

Visual Imitation and Robotic Video Synthesis. A growing line of work closes the loop between generative video models and robot learning [4, 7, 16, 20, 20, 23, 33, 43, 51, 52, 59]. *RIGVid* uses AI-generated task videos (filtered by a VLM), estimates 6-DoF trajectories from the videos, and executes the resulting rollouts on real robots—achieving complex tasks such as pouring and wiping without physical demonstrations [36]. *Gen2Act* generates human execution videos in novel scenes and conditions a *single* policy on those videos to generalize manipulation to unseen objects and motions [3]. Large cross-domain datasets such as BridgeData V2 provide broad task and environment coverage for scalable imitation learning [47]. Compared to methods that rely on heavy end-to-end T2V or expensive data collection, we take a complementary path: starting from a powerful *image* diffusion backbone (DiT), we add parameter-efficient LoRA adapters and explicit text/trajectory conditions to synthesize *robotic manipulation videos* with fine-grained, repeatable motion control, striking a favorable balance between cost, controllability, and generality.

Controllable Generation. Early controllable generation in diffusion exploits *explicit conditioning branches* or *guided objectives* to steer pretrained models. A seminal instance is **ControlNet**, which freezes a text-to-image backbone and adds a zero-initialized control branch to inject spatial conditions (edges, depth, pose), enabling precise composition without degrading the base model [40, 53, 55, 56,

58]. More recently, surveys have systematized controllability along conditioning types (layout/pose/depth/boxes), guidance strategies, and training vs. training-free control for both image and video diffusion [9], highlighting open challenges in multi-condition fusion and temporally consistent control [8]. As representative applications, **GLIGEN** introduces open-set *grounded* generation by injecting region-level grounding (e.g., bounding boxes) via gated adapters while keeping the base diffusion model frozen [24]; on the video side, **Motion Prompting** conditions generation on sparse or dense *point trajectories*, jointly controlling object and camera motion for fine-grained, temporally coherent synthesis [12]. These advances motivate our design to combine LoRA-based parameter-efficient adapters with text/trajectory conditions to achieve repeatable, robot-centric controllability in manipulation videos. Recently, transformer-based diffusion models have enabled semantic and spatial conditions to be represented uniformly as token sequences. These condition tokens are incorporated into the generative process via multimodal attention or concatenation strategies, as seen in DiT-style frameworks such as EasyControl[57]. This token-centric perspective has significantly pushed forward conditional image generation [13, 14, 17, 18, 41, 42, 48, 50], offering better scalability, cleaner architectural design, and more efficient support for diverse or high-resolution conditioning inputs.

3. Method

Our goal is to transform a pretrained image generation model into a controllable *video-like* synthesizer capable of producing short robotic manipulation sequences from minimal conditional inputs. The overall method comprises three major components: (i) an architectural adaptation that integrates LoRA modules into a diffusion transformer backbone for efficient finetuning; (ii) dual conditioning strategies—text-based and trajectory-based—that enable semantic or spatial control of the generated motion; and (iii) a data synthesis pipeline that converts real robot videos into supervision-ready grid-mask pairs. Figure 2 provides an overview of this framework, and Figure 3 details the data construction process.

3.1. Images Sequence Framework

Backbone and Latent Space. We build on **FLUX.1-dev**, a large rectified-flow/transformer generator from Black Forest Labs, deployed via its official implementation and docs. Following latent diffusion/transformer practice, images are encoded to a latent tensor $z = \mathcal{E}(x)$ by a VAE encoder \mathcal{E} and decoded by \mathcal{D} . The generator \mathcal{G}_θ operates on latents and is conditioned by language and/or a rendered trajectory.

Inputs and Outputs. Let $\{I_t\}_{t=1}^9$ denote nine temporally ordered frames, each represented as a matrix $D^{\text{img}_t} \in \mathbb{R}^{m \times n}$. We construct a 3×3 block matrix \mathbf{D} :

$$\mathbf{D} = \begin{bmatrix} D^{\text{img}_1} & D^{\text{img}_2} & D^{\text{img}_3} \\ D^{\text{img}_6} & D^{\text{img}_5} & D^{\text{img}_4} \\ D^{\text{img}_7} & D^{\text{img}_8} & D^{\text{img}_9} \end{bmatrix}, \quad \mathbf{D} \in \mathbb{R}^{3m \times 3n}, \quad D^{\text{img}_t} \in \mathbb{R}^{m \times n}. \quad (1)$$

This spatial arrangement keeps temporally adjacent frames close on the grid, facilitating short-range temporal reasoning via local attention (see Sec. 3.4).

During training, we feed the model a *partially observed* input grid $\tilde{\mathbf{D}}$, in which only the top-left block contains the observed image D^{img_1} , while all other regions are filled with zeros (black pixels):

$$\tilde{\mathbf{D}} = \begin{bmatrix} D^{\text{img}_1} & \mathbf{0} & \mathbf{0} \\ \mathbf{0} & \mathbf{0} & \mathbf{0} \\ \mathbf{0} & \mathbf{0} & \mathbf{0} \end{bmatrix}, \quad (2)$$

Let \mathcal{E} and \mathcal{D} denote the VAE encoder and decoder, and \mathcal{G}_θ the generator conditioned on c . The network predicts the complete 3×3 grid as

$$\hat{\mathbf{D}} = \mathcal{D}\left(\mathcal{G}_\theta(\mathcal{E}(\tilde{\mathbf{D}}); c)\right), \quad (3)$$

LoRA. We adopt the Low-Rank Adaptation (LoRA) technique [15] to finetune the frozen backbone generator \mathcal{G}_θ with a controlled parameter budget. Specifically, for each selected dense projection matrix $W \in \mathbb{R}^{d \times d}$ in the transformer blocks, we reparameterize the update as

$$W' = W + \Delta W, \quad \Delta W = \alpha A B^\top, \quad (4)$$

$$A \in \mathbb{R}^{d \times r}, \quad B \in \mathbb{R}^{d \times r}, \quad r \ll d,$$

so that only A and B are trained while W remains frozen. In our setting, we apply the adapters to the query and value projections in the self-attention layers, as well as the feed-forward projections. This choice is motivated by empirical evidence (e.g., the original LoRA paper) that adaptation in these subspaces suffices for downstream tasks. By constraining adaptation to $O(r d)$ parameters rather than $O(d^2)$, LoRA enables efficient specialization of the image generator to robot-video domains without incurring inference latency or retraining the full model.

3.2. Overall Architecture

The proposed system is designed to convert a pretrained image generator into a controllable robotic video synthesizer, and is composed of three core modules (see Fig. 2 for an overview). First, the *Text-Conditioned Generation* module uses a natural-language instruction together with the first observed robot-environment frame to generate a full 3×3 image grid representing a manipulation sequence. Second,

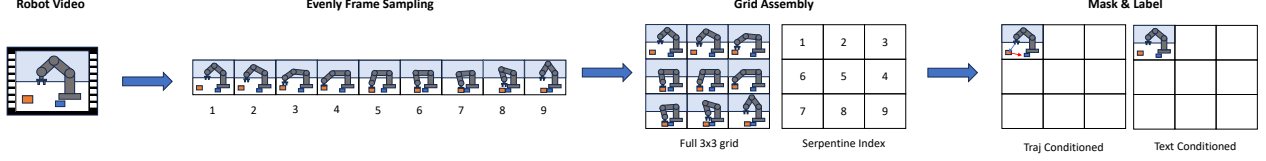


Figure 3. **Data Synthesis Pipeline.** From each robot video, nine frames are uniformly sampled and arranged into a 3×3 grid following a serpentine temporal order ($1 \rightarrow 2 \rightarrow 3, 6 \leftarrow 5 \leftarrow 4, 7 \rightarrow 8 \rightarrow 9$). Only the top-left cell remains visible as the conditioning frame, while the other cells are masked to zero. For the trajectory-conditioned variant, a 2D end-effector path is overlaid on the first frame (red \rightarrow blue indicating temporal progression). The resulting masked grid serves as the model input, and the complete grid as the reconstruction target for supervised training.

the *Trajectory-Conditioned Generation* module accepts a rendered 2D end-effector trajectory over the first frame and synthesizes the corresponding grid, thereby enabling fine-grained spatial motion control. Third, the *Data Synthesis Pipeline* module constructs the training supervision by extracting equi-spaced frames from real robot videos, arranging them into grid layouts, and partitioning the first frame as the visible condition. Together, this architecture enables both semantic control (via text) and spatial control (via trajectory) within a unified generative framework for robotic manipulation video synthesis.

3.3. Conditioning Strategies

In our framework, we support two separate conditioning modalities, each corresponding to a distinct experimental branch: semantic guidance via text, and spatial motion guidance via trajectory. Below we outline each mode and the common inference strategy.

Text-Conditioned Generation. We define a natural-language instruction t (dataset-derived prompt plus a fixed template indicating grid semantics and robot-manipulation context). We embed t using both a CLIP encoder and a T5 tokenizer:

$$e_{\text{clip}} = \text{CLIP}(t)_{\text{pool}}, \quad E_{\text{T5}} = \text{T5}(t) \in \mathbb{R}^{L \times d}, \quad (5)$$

These embeddings are duplicated per generation and injected as conditioning $c_{\text{text}} = \{e_{\text{clip}}, E_{\text{T5}}\}$ into the generator \mathcal{G}_θ via cross-attention. Given the masked input grid \tilde{X} , the generator produces

$$\hat{X} = \mathcal{G}_\theta(\mathcal{E}(\tilde{X}); c_{\text{text}}), \quad (6)$$

and the training follows the latent MSE objective.

Trajectory-Conditioned Generation. In the second branch, we condition the model on a 2D end-effector trajectory $\tau = \{(x_s, y_s)\}_{s=1}^S$ rendered over the first frame I_1 .

We produce the overlay image $I_1^\tau = \text{Overlay}(I_1, \tau)$, and build the masked grid:

$$\tilde{X}^\tau = M \odot \Pi(I_1^\tau, \mathbf{0}, \dots, \mathbf{0}), \quad (7)$$

where only the top-left cell is non-zero. The generator then predicts

$$\hat{X} = \mathcal{G}_\theta(\mathcal{E}(\tilde{X}^\tau); c_\emptyset), \quad (8)$$

This branch emphasizes spatial-motion control while preserving scene semantics from I_1 .

Single-Shot Grid Generation. Rather than performing autoregressive frame generation, both branches employ a single-shot synthesis strategy: the full 3×3 grid is generated at once. This decision takes advantage of the strong compositional priors of image generation models and aligns with observations that such models can implicitly model short temporal sequences via grid layouts.

3.4. Data Synthesis Pipeline

We construct the training supervision from TFDS-stored robot video sequences, including the **JacoPlay**, **BridgeV2**, and **RT-1** datasets. Fig 3 Each episode provides a temporally ordered sequence of RGB frames $\{I_t\}_{t=1}^T$. We uniformly sample 9 frames along the trajectory to form a compact visual summary of the manipulation episode:

$$\{I_t\}_{t=1}^9 = \text{SampleUniform}(\{I_t\}_{t=1}^T, 9), \quad (9)$$

Grid assembly. The sampled frames are arranged into a spatial 3×3 grid image $\mathbf{D} \in \mathbb{R}^{3H \times 3W \times 3}$ through a placement operator Π :

$$\mathbf{D} = \begin{bmatrix} D^{\text{img}_1} & D^{\text{img}_2} & D^{\text{img}_3} \\ D^{\text{img}_6} & D^{\text{img}_5} & D^{\text{img}_4} \\ D^{\text{img}_7} & D^{\text{img}_8} & D^{\text{img}_9} \end{bmatrix}, \quad D^{\text{img}_k} \in \mathbb{R}^{H \times W \times 3}, \quad (10)$$

This *serpentine ordering* ($1 \rightarrow 2 \rightarrow 3, 6 \leftarrow 5 \leftarrow 4, 7 \rightarrow 8 \rightarrow 9$) places temporally adjacent frames in close spatial proximity, helping the transformer’s local attention capture short-range temporal dependencies through neighboring spatial regions.

Masked Input for Conditional generation. During training, we feed the model a *partially observed* input grid $\tilde{\mathbf{D}}$, in which only the top-left block contains the first observed frame, and all other regions are masked to zero (black pixels):

$$\tilde{\mathbf{D}} = \mathbf{M} \odot \mathbf{D}, \quad \mathbf{M}(x, y) = \begin{cases} 1, & \text{if } (x, y) \in \text{block}(D^{\text{img}_1}), \\ 0, & \text{otherwise.} \end{cases} \quad (11)$$

This masked grid provides the conditioning signal for the generator.

Trajectory Overlay. For the trajectory-conditioned branch, we render the 2D end-effector path $\tau = \{(x_s, y_s)\}_{s=1}^S$ directly onto the first frame. Earlier segments are colored **blue**, and later ones **red**, to indicate temporal progression:

$$I_1^\tau = \text{Overlay}(I_1, \tau_{\text{red} \rightarrow \text{blue}}), \quad (12)$$

The overlaid image I_1^τ replaces D^{img_1} in the masked grid, yielding $\tilde{\mathbf{D}}^\tau$.

Supervision Construction. The model is trained to reconstruct the complete ground-truth grid \mathbf{D}_{gt} from the masked condition:

$$\mathcal{L}_{\text{lat}} = \|\mathcal{E}(\mathbf{D}_{gt}) - \mathcal{E}(\tilde{\mathbf{D}})\|_2^2, \quad \hat{\mathbf{D}} = \mathcal{D}\left(\mathcal{G}_\theta(\mathcal{E}(\tilde{\mathbf{D}}); c)\right), \quad (13)$$

This produces paired data $(\tilde{\mathbf{D}}, \mathbf{D}_{gt})$ for text-conditioned training, and $(\tilde{\mathbf{D}}^\tau, \mathbf{D}_{gt})$ for trajectory-conditioned training. After generation, the predicted grid $\hat{\mathbf{D}}$ is split into 9 frames for quantitative evaluation and qualitative visualization.

4. Experiments

4.1. Setup and Implementation

Datasets: JacoPlay, Bridge, RT1 dataset We evaluate on three real-world manipulation datasets.

JacoPlay provides 1,085 teleoperated episodes on a Kinova Jaco arm with clear observations, actions, and natural-language goal annotations; we use the official release for training and evaluation [10].

BridgeData V2 is a large, diverse collection of real robot manipulation trajectories designed for scalable robot learning, comprising 53,896 trajectories across 24 environments; we follow the public CoRL/PMLR release and its splits. We randomly choose 9,967 samples for training and 515 for test [46].

RT-1 accompanies the Robotics Transformer study with a real-world dataset of $\sim 130\text{k}$ episodes spanning 700+ tasks collected by a fleet of 13 robots over 17 months; we cite the RSS'23 publication and project resources. We randomly choose 9,067 samples for training and 698 for test [5].

4.2. Quantitative Results

Evaluation Metrics. We report four standard metrics for video generation and robotic control quality.

Fréchet Video Distance (FVD). FVD measures the Wasserstein-2 (Fréchet) distance between multivariate Gaussians fitted to deep video features of real and generated clips (typically I3D features), capturing both spatial fidelity and temporal coherence [44, 45]. Let (μ_r, Σ_r) and (μ_g, Σ_g) be the empirical mean and covariance of real and generated video features, respectively.

$$\text{FVD} = \|\mu_r - \mu_g\|_2^2 + \text{Tr}\left(\Sigma_r + \Sigma_g - 2(\Sigma_r^{1/2}\Sigma_g\Sigma_r^{1/2})^{1/2}\right), \quad (14)$$

Lower is better. While widely used, recent analyses note potential content biases; thus we also report frame-wise metrics for completeness.

Structural Similarity (SSIM). SSIM assesses perceptual similarity by comparing luminance l , contrast c , and structure s between a generated frame x and its reference y [49]:

$$\text{SSIM}(x, y) = \frac{(2\mu_x\mu_y + C_1)(2\sigma_{xy} + C_2)}{(\mu_x^2 + \mu_y^2 + C_1)(\sigma_x^2 + \sigma_y^2 + C_2)}, \quad (15)$$

where μ and σ are local means and variances, σ_{xy} is the covariance, and C_1, C_2 are stabilizers. Higher is better.

Mean Squared Error (MSE). MSE is the average squared pixel error between a generated frame x and reference y :

$$\text{MSE}(x, y) = \frac{1}{N} \sum_{i=1}^N (x_i - y_i)^2, \quad (16)$$

where N denotes the total number of pixels, and x_i, y_i are the intensity values of the i -th pixel in the generated and reference images, respectively. It serves as a classical full-reference fidelity metric complementary to SSIM [49]. Lower is better.

Success Rate. Following robotics evaluation practice (e.g., RT-1), we compute the proportion of evaluation episodes whose terminal state satisfies a task-specific success predicate defined by the dataset protocol or instruction (e.g., object placed in target receptacle) [6]. Formally, for K trials with binary outcomes $s_k \in \{0, 1\}$,

$$\text{SuccessRate} = \frac{1}{K} \sum_{k=1}^K s_k, \quad (17)$$

Main Results. We evaluate the two experimental branches—*text-conditioned generation* (baseline) and *trajectory-conditioned generation* (our proposed spatial control variant)—across the JacoPlay, BridgeV2, and RT-1 datasets using four complementary metrics mentioned above.

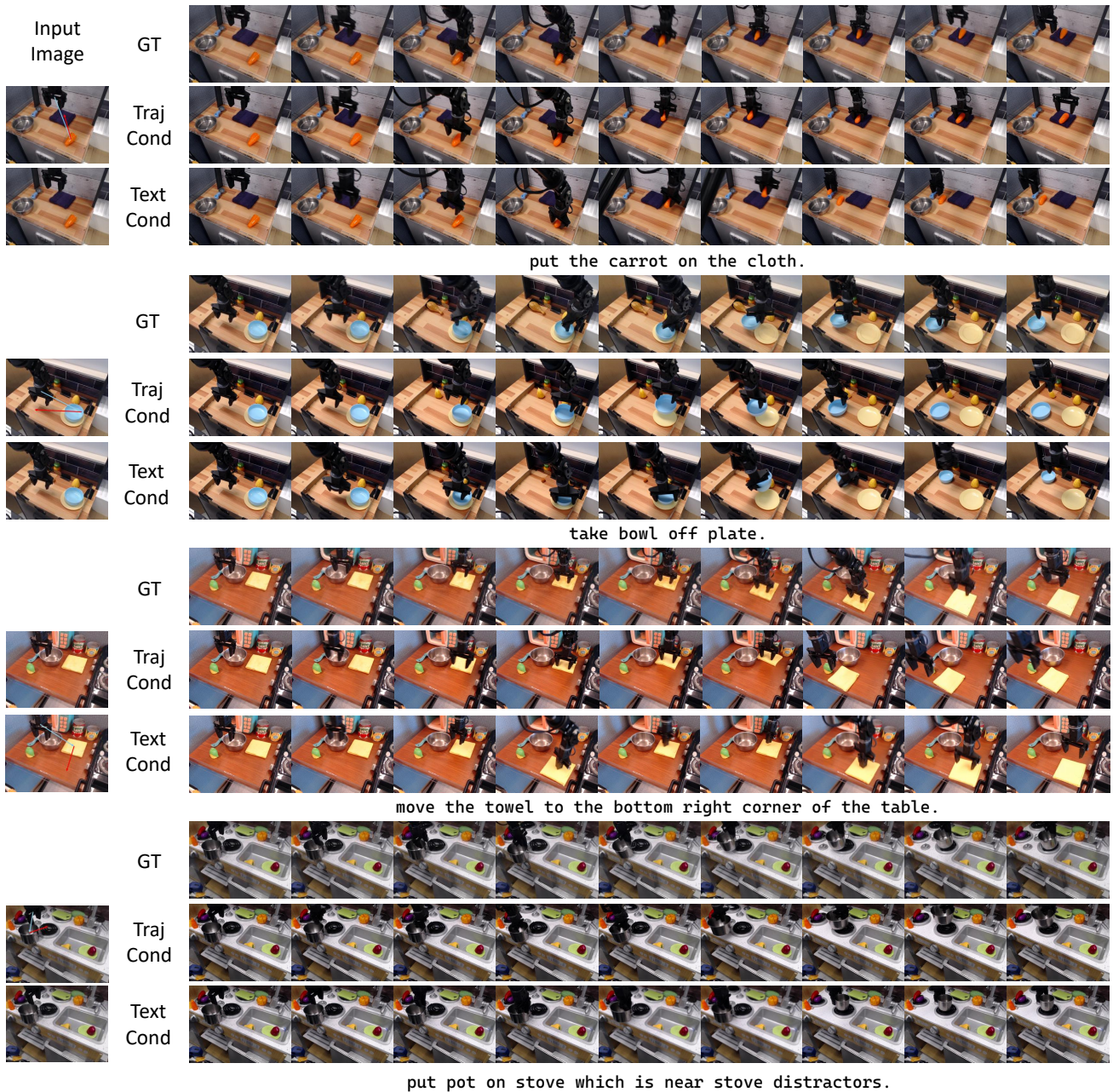


Figure 4. **Qualitative comparisons between text-conditioned and trajectory-conditioned generation.** Each row shows a 9-frame sequence arranged in temporal order. The top example (*put the carrot on the cloth*) and bottom example (*take bowl off plate*) illustrate how both conditioning strategies interpret the same initial frame differently. The text-conditioned model relies solely on semantic understanding of the prompt to identify the correct object and its intended motion, while the trajectory-conditioned model follows the spatial path provided by the overlaid end-effector trace.

4.3. Qualitative Results

We compare the two conditioning modes—*text-conditioned* and *trajectory-conditioned* generation—on representative manipulation tasks. As shown in Fig. 4, the text-

conditioned model excels at semantic grounding: it identifies the correct target object and generates plausible interactions. In contrast, the trajectory-conditioned model emphasizes spatial precision, producing motions that closely follow the provided 2D end-effector path for fine-grained con-

Table 1. **Main results across datasets.** Mean over 100 episodes (3 seeds). FVD↓, SSIM↑, MSE↓, Success↑.

Dataset	Method	FVD↓	SSIM↑	MSE↓	Success↑
JacoPlay	Text	490.7	0.797	0.00695	80.6%
	Traj	503.37	0.802	0.00680	74.0%
BridgeV2	Text	644.2	0.733	0.0135	73.2%
	Traj	693.2	0.726	0.0152	70.9%
RT-1	Text	698.0	0.727	0.0118	72.4%
	Traj	688.1	0.731	0.0117	81.7%

trol. Both modes generate temporally coherent sequences with smooth and physically consistent transitions between actions. The grid-based layout naturally enforces frame-to-frame continuity via local attention, maintaining stable backgrounds and consistent object–arm dynamics across time. Together, these results show that text conditioning contributes semantic intent, while trajectory conditioning provides geometric accuracy.

4.4. Ablation Studies

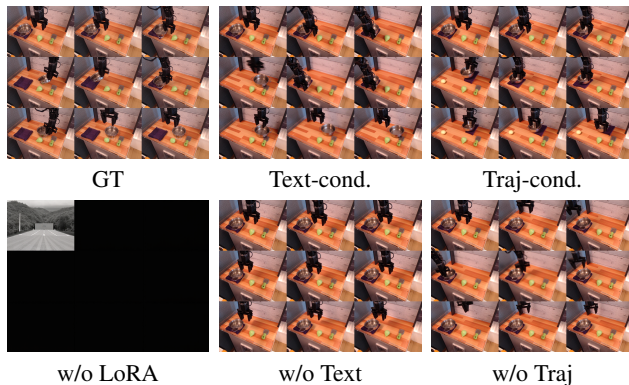


Figure 5. **Ablation on the instruction “place the pot behind the green pear.”** Top: full models with LoRA and correct conditioning. Bottom: removing LoRA or conditioning causes incoherent or aimless motions, while full models complete the instructed placement.

To isolate the contribution of each component, we perform ablations on BridgeV2 while keeping all training settings fixed. Fig 5 Table 2

Effect of LoRA Adaptation. **w/o LoRA (frozen backbone)** tests whether the pretrained generator can synthesize manipulation sequences on its own. The frozen model fails to produce coherent grids, showing that general image priors alone do not transfer to robot-motion generation. LoRA is therefore essential for injecting task-specific motion and interaction semantics with minimal parameters.

Table 2. **Ablation results on BridgeV2.** Each ablation modifies a single component from the full model. ↓ lower is better; ↑ higher is better.

Configuration	FVD↓	SSIM↑	MSE↓	Success↑
Full model (Traj, grid)	644.2	0.733	0.0135	73.2%
Full model (Text, grid)	693.2	0.726	0.0152	70.9%
w/o LoRA (frozen backbone)	4377.1	0.064	0.1785	0%
w/o Prompt Template (Text)	843.4	0.754	0.0153	2.5%
w/o Trajectory Overlay (Traj)	720.0	0.749	0.0157	3.9%

Effect of Text Prompt Templates. Using raw dataset instructions (no template) noticeably degrades image quality and alignment. Without explicit cues about grid structure and manipulation intent, the arm often moves aimlessly and fails to pick the correct object, demonstrating that prompt structure meaningfully improves semantic grounding.

Effect of Trajectory Overlay. Removing rendered 2D trajectory from the trajectory-conditioned branch leads to clear failures: arm motions drift, objects barely move, and the model no longer executes the intended spatial path. This confirms that the visual trajectory overlay provides crucial spatial conditioning for precise, target-directed motion.

4.5. Failure Cases and Limitations

Our method remains stable across diverse scenes, but we occasionally observe minor visual inconsistencies. Slight tone or texture variations may appear between grid tiles due to independent latent sampling, and in rare cases, mild misalignment can occur along tile boundaries. These effects are visually negligible and do not affect the semantic correctness or temporal coherence of the generated manipulation sequences.

5. Conclusion

We have presented a controllable robotic video synthesis framework that adapts a pretrained image generator into a video-like model through lightweight LoRA adaptation. By reformulating robot manipulation sequences as 3×3 grid images, our approach unifies text- and trajectory-conditioned generation within a single architecture, leveraging the compositional priors of large image models for temporal reasoning. Experiments on multiple robot datasets demonstrate that the model not only generates coherent and physically plausible motion but also achieves competitive quantitative performance under both semantic and spatial conditioning.

Beyond these results, our study highlights a broader insight: high-capacity image generators, when properly conditioned and adapted, can serve as visual planners capable of synthesizing action-consistent manipulation sequences from static inputs.

References

- [1] Philip J. Ball, J. Bauer, F. Belletti, et al. Genie 3: A new frontier for world models, 2025. 3
- [2] Omer Bar-Tal, Hila Chefer, Omer Tov, Charles Herrmann, Roni Paiss, Shiran Zada, Ariel Ephrat, Junhwa Hur, Guanghui Liu, Amit Raj, Yuanzhen Li, Michael Rubinstein, Tomer Michaeli, Oliver Wang, Deqing Sun, Tali Dekel, and Inbar Mosseri. Lumiere: A space-time diffusion model for video generation. *arXiv preprint arXiv:2401.12945*, 2024. A SIGGRAPH Asia 2024 Technical Communications version is available. 3
- [3] Homanga Bharadhwaj, Debidatta Dwibedi, Abhinav Gupta, Shubham Tulsiani, Carl Doersch, Ted Xiao, Dhruv Shah, Fei Xia, Dorsa Sadigh, and Sean Kirmani. Gen2act: Human video generation in novel scenarios enables generalizable robot manipulation. In *Proceedings of the Conference on Robot Learning (CoRL)*, 2025. Project: <https://homangab.github.io/gen2act/>. 3
- [4] Kevin Black, Noah Brown, Danny Driess, Adnan Esmail, Michael Equi, Chelsea Finn, Niccolo Fusai, Lachy Groom, Karol Hausman, Brian Ichter, Szymon Jakubczak, Tim Jones, Liyiming Ke, Sergey Levine, Adrian Li-Bell, Mohith Mothukuri, Suraj Nair, Karl Pertsch, Lucy Xiaoyang Shi, James Tanner, Quan Vuong, Anna Walling, Haohuan Wang, and Ury Zhilinsky. π_0 : A vision-language-action flow model for general robot control, 2024. 3
- [5] Anthony Brohan, Noah Brown, Justice Carbajal, Yevgen Chebotar, Joseph Dabis, Chelsea Finn, Keerthana Gopalakrishnan, Karol Hausman, Alexander Herzog, Jasmine Hsu, Julian Ibarz, Brian Ichter, Alex Irpan, Tomas Jackson, Sally Jesmonth, Nikhil Joshi, Ryan Julian, Dmitry Kalashnikov, Yuheng Kuang, Isabel Leal, Kuang-Huei Lee, Sergey Levine, Yao Lu, Utsav Malla, Deeksha Manjunath, Igor Mordatch, Ofir Nachum, Carolina Parada, Jodilyn Peralta, Emily Perez, Karl Pertsch, Jornell Quiambao, Kanishka Rao, Michael S Ryoo, Grecia Salazar, Pannag R Sanketi, Kevin Sayed, Jaspiar Singh, Sumedh Sontakke, Austin Stone, Clayton Tan, Huong Tran, Vincent Vanhoucke, Steve Vega, Quan H Vuong, Fei Xia, Ted Xiao, Peng Xu, Sichun Xu, Tianhe Yu, and Brianna Zitkovich. RT-1: Robotics Transformer for Real-World Control at Scale. In *Proceedings of Robotics: Science and Systems*, Daegu, Republic of Korea, 2023. 6
- [6] Anthony Brohan, Noah Brown, Justice Carbajal, Yevgen Chebotar, Joseph Dabis, Chelsea Finn, Keerthana Gopalakrishnan, Karol Hausman, Alexander Herzog, Jasmine Hsu, Julian Ibarz, Brian Ichter, Alex Irpan, Tomas Jackson, Sally Jesmonth, Nikhil Joshi, Ryan Julian, Dmitry Kalashnikov, Yuheng Kuang, Isabel Leal, Kuang-Huei Lee, Sergey Levine, Yao Lu, Utsav Malla, Deeksha Manjunath, Igor Mordatch, Ofir Nachum, Carolina Parada, Jodilyn Peralta, Emily Perez, Karl Pertsch, Jornell Quiambao, Kanishka Rao, Michael S. Ryoo, Grecia Salazar, Pannag R. Sanketi, Kevin Sayed, Jaspiar Singh, Sumedh Sontakke, Austin Stone, Clayton Tan, Huong Tran, Vincent Vanhoucke, Steve Vega, Quan H. Vuong, Fei Xia, Ted Xiao, Peng Xu, Sichun Xu, Tianhe Yu, and Brianna Zitkovich. Rt-1: Robotics transformer for real-world control at scale. In *Proceedings of Robotics: Science and Systems (RSS)*, Daegu, Republic of Korea, 2023. 6
- [7] Anthony Brohan, Noah Brown, Justice Carbajal, Yevgen Chebotar, Joseph Dabis, Chelsea Finn, Keerthana Gopalakrishnan, Karol Hausman, Alex Herzog, Jasmine Hsu, Julian Ibarz, Brian Ichter, Alex Irpan, Tomas Jackson, Sally Jesmonth, Nikhil J Joshi, Ryan Julian, Dmitry Kalashnikov, Yuheng Kuang, Isabel Leal, Kuang-Huei Lee, Sergey Levine, Yao Lu, Utsav Malla, Deeksha Manjunath, Igor Mordatch, Ofir Nachum, Carolina Parada, Jodilyn Peralta, Emily Perez, Karl Pertsch, Jornell Quiambao, Kanishka Rao, Michael Ryoo, Grecia Salazar, Pannag Sanketi, Kevin Sayed, Jaspiar Singh, Sumedh Sontakke, Austin Stone, Clayton Tan, Huong Tran, Vincent Vanhoucke, Steve Vega, Quan Vuong, Fei Xia, Ted Xiao, Peng Xu, Sichun Xu, Tianhe Yu, and Brianna Zitkovich. Rt-1: Robotics transformer for real-world control at scale, 2023. 3
- [8] Puyang Cao, Yang Zhou, et al. Controllable generation with text-to-image diffusion models: A survey. *arXiv preprint arXiv:2403.04279*, 2024. 4
- [9] Xuewei Chen, Zhimin Chen, and Yiren Song. Transanimate: Taming layer diffusion to generate rgba video. *arXiv preprint arXiv:2503.17934*, 2025. 4
- [10] Shivin Dass, Jullian Yapeter, Jesse Zhang, Jiahui Zhang, Karl Pertsch, Stefanos Nikolaidis, and Joseph J. Lim. Clvr jaco play dataset, 2023. 6
- [11] Google Deepmind. Veo 3. <https://deepmind.google/technologies/veo/veo-3/>, 2025. Accessed: 2025-11-08. 3
- [12] Di Geng, Yuwei Lin, Danelljan Xu, Tim Meinhardt, Songhua Lu, Martin Danelljan, et al. Controlling video generation with motion trajectories. *arXiv preprint arXiv:2412.02700*, 2025. CVPR 2025 (to appear). 3, 4
- [13] Yan Gong, Yiren Song, Yicheng Li, Chenglin Li, and Yin Zhang. Relationadapter: Learning and transferring visual relation with diffusion transformers. *arXiv preprint arXiv:2506.02528*, 2025. 4
- [14] Hailong Guo, Bohan Zeng, Yiren Song, Wentao Zhang, Chuang Zhang, and Jiaming Liu. Any2anytron: Leveraging adaptive position embeddings for versatile virtual clothing tasks. *arXiv preprint arXiv:2501.15891*, 2025. 4
- [15] Edward J. Hu, Yelong Shen, Phillip Wallis, Zeyuan Allen-Zhu, Yuanzhi Li, Shean Wang, Lu Wang, and Weizhu Chen. Lora: Low-rank adaptation of large language models. *arXiv preprint arXiv:2106.09685*, 2021. 2, 4
- [16] Jiangyong Huang, Silong Yong, Xiaojian Ma, Xiongkun Linghu, Puhao Li, Yan Wang, Qing Li, Song-Chun Zhu, Baoxiong Jia, and Siyuan Huang. An embodied generalist agent in 3d world, 2024. 3
- [17] Shijie Huang, Yiren Song, Yuxuan Zhang, Hailong Guo, Xueyin Wang, Mike Zheng Shou, and Jiaming Liu. Photodoodle: Learning artistic image editing from few-shot pairwise data. *arXiv preprint arXiv:2502.14397*, 2025. 4
- [18] Yuxin Jiang, Yuchao Gu, Yiren Song, Ivor Tsang, and Mike Zheng Shou. Personalized vision via visual in-context learning. *arXiv preprint arXiv:2509.25172*, 2025. 4

- [19] Yang Jin, Zhicheng Sun, Ningyuan Li, Kun Xu, Kun Xu, Hao Jiang, Nan Zhuang, Quzhe Huang, Yang Song, Yadong Mu, and Zhouchen Lin. Pyramidal flow matching for efficient video generative modeling, 2025. 3
- [20] Moo Jin Kim, Karl Pertsch, Siddharth Karamcheti, Ted Xiao, Ashwin Balakrishna, Suraj Nair, Rafael Rafailov, Ethan Foster, Grace Lam, Pannag Sanketi, Quan Vuong, Thomas Kolmar, Benjamin Burchfiel, Russ Tedrake, Dorsa Sadigh, Sergey Levine, Percy Liang, and Chelsea Finn. Openvla: An open-source vision-language-action model, 2024. 3
- [21] Weijie Kong, Qi Tian, Zijian Zhang, Rox Min, Zuozhuo Dai, Jin Zhou, Jiangfeng Xiong, Xin Li, Bo Wu, Jianwei Zhang, Kathrina Wu, Qin Lin, Junkun Yuan, Yanxin Long, Aladdin Wang, Andong Wang, Changlin Li, DuoJun Huang, Fang Yang, Hao Tan, Hongmei Wang, Jacob Song, Jiawang Bai, Jianbing Wu, Jinbao Xue, Joey Wang, Kai Wang, Mengyang Liu, Pengyu Li, Shuai Li, Weiyan Wang, Wenqing Yu, Xincheng Deng, Yang Li, Yi Chen, Yutao Cui, Yuanbo Peng, Zhentao Yu, Zhiyu He, Zhiyong Xu, Zixiang Zhou, Zunnan Xu, Yangyu Tao, Qinglin Lu, Songtao Liu, Dax Zhou, Hongfa Wang, Yong Yang, Di Wang, Yuhong Liu, Jie Jiang, and Caesar Zhong. Hunyuanvideo: A systematic framework for large video generative models, 2025. 3
- [22] Pengxiang Li, Kai Chen, Zhili Liu, Ruiyuan Gao, Lanqing Hong, Dit-Yan Yeung, Huchuan Lu, and Xu Jia. Trackdiffusion: Tracklet-conditioned video generation via diffusion models. In *Proceedings of the IEEE/CVF Winter Conference on Applications of Computer Vision (WACV)*, pages 3539–3548, 2025. 3
- [23] Xinghang Li, Minghuan Liu, Hanbo Zhang, Cunjun Yu, Jie Xu, Hongtao Wu, Chilam Cheang, Ya Jing, Weinan Zhang, Huaping Liu, Hang Li, and Tao Kong. Vision-language foundation models as effective robot imitators, 2024. 3
- [24] Yuheng Li, Haotian Liu, Qingyang Wu, Fangzhou Mu, Jianwei Yang, Jianfeng Gao, Chunyuan Li, and Yong Jae Lee. Gligen: Open-set grounded text-to-image generation. In *Proceedings of the IEEE/CVF Conference on Computer Vision and Pattern Recognition (CVPR)*, 2023. 4
- [25] Yue Ma, Hongyu Liu, Hongfa Wang, Heng Pan, Yingqing He, Junkun Yuan, Ailing Zeng, Chengfei Cai, Heung-Yeung Shum, Wei Liu, et al. Follow-your-emoji: Fine-controllable and expressive freestyle portrait animation. In *SIGGRAPH Asia 2024 Conference Papers*, pages 1–12, 2024. 3
- [26] Yue Ma, Kunyu Feng, Zhongyuan Hu, Xinyu Wang, Yucheng Wang, Mingzhe Zheng, Xuanhua He, Chenyang Zhu, Hongyu Liu, Yingqing He, et al. Controllable video generation: A survey. *arXiv preprint arXiv:2507.16869*, 2025.
- [27] Yue Ma, Kunyu Feng, Xinhua Zhang, Hongyu Liu, David Junhao Zhang, Jinbo Xing, Yinhan Zhang, Ayden Yang, Zeyu Wang, and Qifeng Chen. Follow-your-creation: Empowering 4d creation through video inpainting. *arXiv preprint arXiv:2506.04590*, 2025.
- [28] Yue Ma, Yingqing He, Hongfa Wang, Andong Wang, Leqi Shen, Chenyang Qi, Jixuan Ying, Chengfei Cai, Zhifeng Li, Heung-Yeung Shum, et al. Follow-your-click: Open-domain regional image animation via motion prompts. In *Proceedings of the AAAI Conference on Artificial Intelligence*, pages 6018–6026, 2025.
- [29] Yue Ma, Yulong Liu, Qiyuan Zhu, Ayden Yang, Kunyu Feng, Xinhua Zhang, Zhifeng Li, Sirui Han, Chenyang Qi, and Qifeng Chen. Follow-your-motion: Video motion transfer via efficient spatial-temporal decoupled finetuning. *arXiv preprint arXiv:2506.05207*, 2025.
- [30] Yue Ma, Zexuan Yan, Hongyu Liu, Hongfa Wang, Heng Pan, Yingqing He, Junkun Yuan, Ailing Zeng, Chengfei Cai, Heung-Yeung Shum, et al. Follow-your-emoji-faster: Towards efficient, fine-controllable, and expressive freestyle portrait animation. *arXiv preprint arXiv:2509.16630*, 2025. 3
- [31] Andrew Melnik, Michal Ljubljanac, Cong Lu, Qi Yan, Weiming Ren, and Helge Ritter. Video diffusion models: A survey. *arXiv preprint arXiv:2405.03150*, 2024. 3
- [32] Minimax. Hailuo. <https://hailuoai.com/video>, 2024. Accessed: 2025-11-08. 3
- [33] NVIDIA, :, Johan Bjorck, Fernando Castañeda, Nikita Cherniadev, Xingye Da, Runyu Ding, Linxi "Jim" Fan, Yu Fang, Dieter Fox, Fengyuan Hu, Spencer Huang, Joel Jang, Zhenyu Jiang, Jan Kautz, Kaushil Kundalia, Lawrence Lao, Zhiqi Li, Zongyu Lin, Kevin Lin, Guilin Liu, Edith Llon-top, Loic Magne, Ajay Mandlekar, Avnish Narayan, Soroush Nasiriany, Scott Reed, You Liang Tan, Guanzhi Wang, Zu Wang, Jing Wang, Qi Wang, Jiannan Xiang, Yuqi Xie, Yinzhen Xu, Zhenjia Xu, Seonghyeon Ye, Zhiding Yu, Ao Zhang, Hao Zhang, Yizhou Zhao, Ruijie Zheng, and Yuke Zhu. Gr00t n1: An open foundation model for generalist humanoid robots, 2025. 3
- [34] OpenAI. Video generation models as world simulators. <https://openai.com/index/video-generation-models-as-world-simulators/>, 2024. Accessed: 2025-10-28. 3
- [35] OpenAI. Sora. <https://openai.com/sora/>, 2024. Accessed: 2025-11-08. 3
- [36] Shivansh Patel, Shraddha Mohan, Svetlana Lazebnik, et al. Robotic manipulation by imitating generated videos (rigvid). *arXiv preprint arXiv:2507.00990*, 2025. Project page: <https://rigvid-robot.github.io/>. 3
- [37] William Peebles and Saining Xie. Scalable diffusion models with transformers. In *Proceedings of the IEEE/CVF International Conference on Computer Vision (ICCV)*, pages 4195–4205, 2023. 3
- [38] Adam Polyak, Amit Zohar, Andrew Brown, Andros Tjandra, Animesh Sinha, Ann Lee, Apoorv Vyas, Bowen Shi, Chih-Yao Ma, Ching-Yao Chuang, David Yan, Dhruv Choudhary, Dingkang Wang, Geet Sethi, Guan Pang, Haoyu Ma, Ishan Misra, Ji Hou, Jialiang Wang, Kiran Jagadeesh, Kunpeng Li, Luxin Zhang, Mannat Singh, Mary Williamson, Matt Le, Matthew Yu, Mitesh Kumar Singh, Peizhao Zhang, Peter Vajda, Quentin Duval, Rohit Girdhar, Roshan Sumbaly, Sai Saketh Rambhatla, Sam Tsai, Samaneh Azadi, Samyak Datta, Sanyuan Chen, Sean Bell, Sharadh Ramaswamy, Shelly Sheynin, Siddharth Bhattacharya, Simran Motwani, Tao Xu, Tianhe Li, Tingbo Hou, Wei-Ning Hsu, Xi Yin, Xiaoliang Dai, Yaniv Taigman, Yaqiao Luo, Yen-Cheng Liu,

- Yi-Chiao Wu, Yue Zhao, Yuval Kirstain, Zecheng He, Zijian He, Albert Pumarola, Ali Thabet, Artsiom Sanakoyeu, Arun Mallya, Baishan Guo, Boris Araya, Breena Kerr, Carleigh Wood, Ce Liu, Cen Peng, Dmitry Vengertsev, Edgar Schonfeld, Elliot Blanchard, Felix Juefei-Xu, Fraylie Nord, Jeff Liang, John Hoffman, Jonas Kohler, Kaolin Fire, Karthik Sivakumar, Lawrence Chen, Licheng Yu, Luya Gao, Markos Georgopoulos, Rashed Moritz, Sara K. Sampson, Shikai Li, Simone Parmeggiani, Steve Fine, Tara Fowler, Vladan Petrovic, and Yuming Du. Movie gen: A cast of media foundation models, 2025. 3
- [39] Runway. Gen 3. <https://runwayml.com/research/introducing-gen-3-alpha>, 2024. Accessed: 2025-11-08. 3
- [40] Yiren Song, Shijie Huang, Chen Yao, Xiaojun Ye, Hai Ci, Jiaming Liu, Yuxuan Zhang, and Mike Zheng Shou. Processpainter: Learn painting process from sequence data. *arXiv preprint arXiv:2406.06062*, 2024. 3
- [41] Yiren Song, Danze Chen, and Mike Zheng Shou. Layer-tracer: Cognitive-aligned layered svg synthesis via diffusion transformer. *arXiv preprint arXiv:2502.01105*, 2025. 4
- [42] Yiren Song, Cheng Liu, and Mike Zheng Shou. Makeanything: Harnessing diffusion transformers for multi-domain procedural sequence generation. *arXiv preprint arXiv:2502.01572*, 2025. 4
- [43] Octo Model Team, Dibya Ghosh, Homer Walke, Karl Pertsch, Kevin Black, Oier Mees, Sudeep Dasari, Joey Hejna, Tobias Kreiman, Charles Xu, Jianlan Luo, You Liang Tan, Lawrence Yunliang Chen, Pannag Sanketi, Quan Vuong, Ted Xiao, Dorsa Sadigh, Chelsea Finn, and Sergey Levine. Octo: An open-source generalist robot policy, 2024. 3
- [44] Thomas Unterthiner, Sjoerd van Steenkiste, Karol Kurach, Raphaël Marinier, Marcin Michalski, and Sylvain Gelly. Towards accurate generative models of video: A new metric & challenges. *arXiv*, 2018. 6
- [45] Thomas Unterthiner, Sjoerd van Steenkiste, Karol Kurach, Raphaël Marinier, Marcin Michalski, and Sylvain Gelly. Fvd: A new metric for video generation. In *Deep Generative Models for Highly Structured Data (DGS) @ ICLR*, 2019. 6
- [46] Homer Rich Walke, Kevin Black, Tony Z. Zhao, Quan Vuong, Chongyi Zheng, Philippe Hansen-Estruch, Andre Wang He, Vivek Myers, Moo Jin Kim, Max Du, Abraham Lee, Kuan Fang, Chelsea Finn, and Sergey Levine. Bridgedata v2: A dataset for robot learning at scale. In *Proceedings of The 7th Conference on Robot Learning*, pages 1723–1736. PMLR, 2023. 6
- [47] Homer Rich Walke, Kevin Black, Tony Z. Zhao, Quan Vuong, Chongyi Zheng, Philippe Hansen-Estruch, Andre Wang He, Vivek Myers, Moo Jin Kim, Max Du, Abraham Lee, Kuan Fang, Chelsea Finn, and Sergey Levine. Bridgedata v2: A dataset for robot learning at scale. In *Proceedings of The 7th Conference on Robot Learning (CoRL), Proceedings of Machine Learning Research (PMLR)*, pages 1723–1736, 2023. 3
- [48] Cong Wan, Xiangyang Luo, Zijian Cai, Yiren Song, Yunlong Zhao, Yifan Bai, Yuhang He, and Yihong Gong. Grid: Visual layout generation. *arXiv preprint arXiv:2412.10718*, 2024. 4
- [49] Zhou Wang, Alan C. Bovik, Hamid R. Sheikh, and Eero P. Simoncelli. Image quality assessment: From error visibility to structural similarity. *IEEE Transactions on Image Processing*, 13(4):600–612, 2004. 6
- [50] Zitong Wang, Hang Zhao, Qianyu Zhou, Xuequan Lu, Xi-angtai Li, and Yiren Song. Diffdecompose: Layer-wise decomposition of alpha-composited images via diffusion transformers. *arXiv preprint arXiv:2505.21541*, 2025. 4
- [51] Junjie Wen, Yichen Zhu, Jinming Li, Minjie Zhu, Kun Wu, Zhiyuan Xu, Ning Liu, Ran Cheng, Chaomin Shen, Yaxin Peng, Feifei Feng, and Jian Tang. Tinyvla: Towards fast, data-efficient vision-language-action models for robotic manipulation, 2025. 3
- [52] Hongtao Wu, Ya Jing, Chilam Cheang, Guangzeng Chen, Jiafeng Xu, Xinghang Li, Minghuan Liu, Hang Li, and Tao Kong. Unleashing large-scale video generative pre-training for visual robot manipulation, 2023. 3
- [53] Lvmin Zhang, Anyi Rao, and Maneesh Agrawala. Adding conditional control to text-to-image diffusion models. *arXiv preprint arXiv:2302.05543*, 2023. 3
- [54] Shiwei Zhang, Jiayu Wang, Yingya Zhang, Kang Zhao, Hangjie Yuan, Zhiwu Qin, Xiang Wang, Deli Zhao, and Jingren Zhou. I2vgen-xl: High-quality image-to-video synthesis via cascaded diffusion models, 2023. 3
- [55] Yuxuan Zhang, Yiren Song, Jiaming Liu, Rui Wang, Jinpeng Yu, Hao Tang, Huaxia Li, Xu Tang, Yao Hu, Han Pan, et al. Ssr-encoder: Encoding selective subject representation for subject-driven generation. In *Proceedings of the IEEE/CVF Conference on Computer Vision and Pattern Recognition*, pages 8069–8078, 2024. 3
- [56] Yuxuan Zhang, Lifu Wei, Qing Zhang, Yiren Song, Jiaming Liu, Huaxia Li, Xu Tang, Yao Hu, and Haibo Zhao. Stablemakeup: When real-world makeup transfer meets diffusion model. *arXiv preprint arXiv:2403.07764*, 2024. 3
- [57] Yuxuan Zhang, Yirui Yuan, Yiren Song, Haofan Wang, and Jiaming Liu. Easycontrol: Adding efficient and flexible control for diffusion transformer. *arXiv preprint arXiv:2503.07027*, 2025. 4
- [58] Yuxuan Zhang, Qing Zhang, Yiren Song, Jichao Zhang, Hao Tang, and Jiaming Liu. Stable-hair: Real-world hair transfer via diffusion model. In *Proceedings of the AAAI Conference on Artificial Intelligence*, pages 10348–10356, 2025. 4
- [59] Jinliang Zheng, Jianxiong Li, Dongxiu Liu, Yinan Zheng, Zhihao Wang, Zhonghong Ou, Yu Liu, Jingjing Liu, Ya-Qin Zhang, and Xianyuan Zhan. Universal actions for enhanced embodied foundation models, 2025. 3